



A Synergic Activity of Urea/Butyl Imidazolium Ionic Liquid Supported on UiO-66-NH₂ Metal–Organic Framework for Synthesis of Oximes

Saeed Askari¹ · Mohammad Jafarzadeh¹ · David Benjamin Christensen² · Søren Kegnæs²

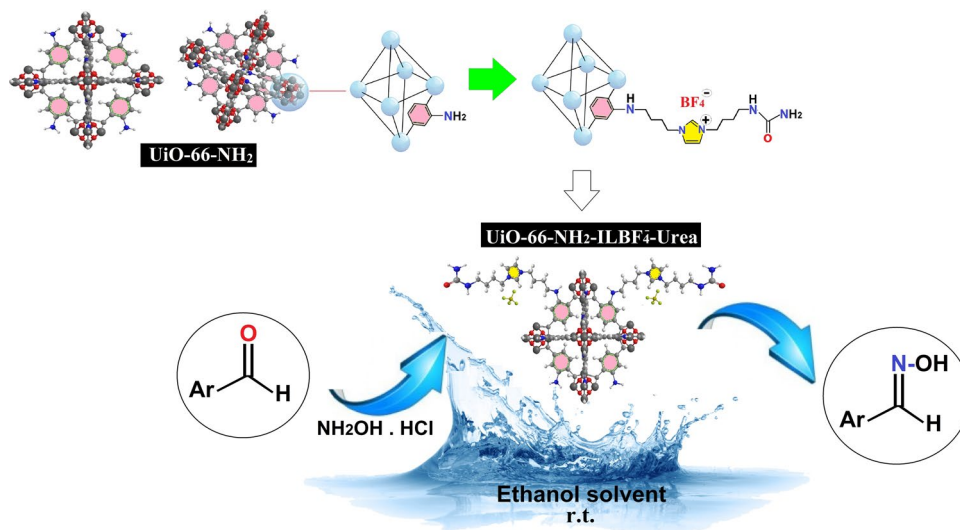
Received: 11 February 2020 / Accepted: 27 March 2020
© Springer Science+Business Media, LLC, part of Springer Nature 2020

Abstract

An efficient supported ionic liquid catalyst is designed for condensation reaction of aldehydes and ketones. The Zr-based metal–organic framework (MOF), UiO-66-NH₂, was initially functionalized with *N,N'*-dibutyl imidazolium ionic liquid (UiO-66-NH₂-ILBr⁻), and then urea was attached to the ionic liquid (IL) to form a task-specific IL. Bromide was exchanged with tetrafluoroborate and the catalyst exhibits excellent performance for the synthesis of oximes. The ionic liquid/urea coupling showed a synergistic effect on the efficiency of the reaction. The supported catalyst system was recycled simply by filtration and reused for five times without significant decrease in its activity. The catalyst was characterized with PXRD, FTIR, TGA, XPS, BET, FE-SEM, EDS, elemental mapping and elemental analysis (CHN).

Graphic Abstract

MOF/IL/urea catalytic system was used for the synthesis of oximes



Keywords Supported ionic-liquid phase · Metal–organic frameworks · UiO-66-NH₂ · Oxime synthesis

Electronic supplementary material The online version of this article (<https://doi.org/10.1007/s10562-020-03203-1>) contains supplementary material, which is available to authorized users.

✉ Mohammad Jafarzadeh
m.jafar@razi.ac.ir

Extended author information available on the last page of the article

1 Introduction

Supported ionic liquids (SILs) and supported ionic liquid phase (SILPs) have attracted some interests due to their unique properties and activities compared to conventional ionic liquids (ILs) [1, 2]. A SILP material is defined as a thin and multilayer film (a few nanometer thick) of the ionic

liquid physisorbed on the surface of porous materials [3], while in SILs a monolayer of an ionic liquid is covalently immobilized on the surface (sometimes called as supported ionic liquid-like phase; SILLP) [1]. These concepts diminish the typical issue of the ILs such as high cost, large volume usage, high viscosity (cause difficulty in mass transfer and reactant diffusion) [4], and the need for liquid–liquid extraction for their recovery. Heterogenization of ILs on support materials (e.g. silica, alumina, titania, activated carbon, polymer) [5–7] not only reduce the amount of ionic liquid, provide short diffusion distance (due to a nanometer thickness) [4], makes for easier handling, recycling and long-term stability of ionic liquids [6], and reduce potential risk to the environment due their poor biodegradability [1], but also promotes the performance of the hybrid materials in their applications [6].

Although, SILPs have some advantages such as easy preparation and simple operation particularly in fixed-bed reactors for gas phase reactions, but they suffer from pore blocking and instability in the reaction medium especially in liquid phase. The IL can be removed from the surface (leaching) by force of mechanical stirring and/or dissolving in reaction media [1, 8, 9]. In contrast, by covalent grafting of ILs to the functional groups on the surface of the support, the stability and durability of SILs in organic syntheses may improve significantly. SILs have been used as hosts for organocatalysts [10], metal-complexes [8], and metal nanoparticles [6, 11] and generated task-specific ionic liquids (TSILs) [12–15] and specifically the concept of supported ionic liquid catalysts (SILC) [9, 16–18]. Metal–organic frameworks (MOFs), as class of promising porous materials, have been employed as suitable supports for immobilizing ILs [19, 20] and catalysts [21, 22] due to their high surface area, large pore volume, and available/accessible pores [23]. A synergic effect arising from their hybridization have previously been shown to enhance the efficiency of the catalytic reactions [19, 20]. MOF/TSIL hybrid materials have been used for various organic reactions such as acetalization of benzaldehydes with glycol [24], selective oxidation of cyclohexenes [25] and benzyl alcohols [26, 27], adsorptive desulfurization [28, 29], Knoevenagel condensation [30], cycloaddition of CO₂ with epoxides [31–33] and synthesis of biodiesels [34].

Oximes are important intermediates for synthesis of nitriles [35], amides (Beckmann rearrangement) [36–38], nitrones, hydroximinoyl chlorides, and chiral α -sulfinyl oximes [39]. They are also used for preparation of carbonyl compounds [40] and metal complexes [41], protecting carbonyl compounds, inhibiting enzymes [42] and manufacturing of pharmaceutical products and insecticides [43]. Although various methods have been developed recently for the synthesis of oximes such as decomposition of tosylhydrazones [44], oxidation of methylarenes (in the presence

of a nitrogen source) [45], oxidation of primary amines [46], ammoximation of different ketones and aldehydes using polyoxometalates [47, 48], and transoximation [49], but the conventional method is still considered due to the simplicity of the procedure. Oximes are generally synthesized via a condensation reaction of carbonyl compounds (aldehydes and ketones) with hydroxylamine in acidic or basic conditions [50]. Since hydroxylamine is dangerous to handle and use [51], hydroxylamine hydrochloride is generally employed to generate in-situ hydroxylamine in the reaction medium, with only water and HCl as by-products [50]. Besides conventional conditions for the synthesis of oximes, microwave-assisted [52], ultrasonic [42], and mechanochemical [53] methods have been also developed. ILs have found much interest as an alternative reaction media for the synthesis of oximes [54–56]. It is expected that the application of SILs in the synthesis of oximes can find some benefits in an aspect of economic and environment.

In the present work, zirconium-based MOF, UiO-66-NH₂, is modified by a post-synthesis with imidazolium bromide (ILBr⁻) for the preparation of supported ionic liquid on the surface of the MOF. The SIL was further functionalized with urea to prepare a TSIL. Urea offers basic sites and hydrogen bond donors [57] for catalyzing organic synthesis of oximes, similar to the glycine-catalyzed synthesis in the previous report [58]. However, the urea-functionalized SIL serves as a catalyst and medium in this work. It is expected that the functionalized MOF exhibits heterogeneous characteristics for the IL and the base.

2 Experimental

2.1 Synthesis of 1,3-Bis-(4-bromo-butyl)-3H-imidazol-1-ium Bromide (ILBr⁻)

The preparation of the ionic liquid was adopted from a previously reported method [59]. Imidazole (290 mg, 4.3 mmol) was dissolved in THF (4 mL), and then a solution of sodium hydride (135 mg, 5 mmol) in THF (3 mL) was slowly added at 0 °C. After 45 min of stirring at room temperature, 1,4-dibromobutane (0.51 mL, 4.3 mmol) was added slowly to the above solution and stirred for 2 days. The product was extracted from the reaction mixture using ethyl acetate. In the second step, the product was dissolved in THF and stirred for 45 min. 1,4-dibromobutane (0.55 mL, 4.6 mmol) was then added into the mixture and refluxed for 2 days. The final product was isolated by extraction using ethyl acetate. The products were identified by ¹H and ¹³C NMR and the spectra were compared with data for a similar structure [60] (refer to Supporting Information for details).

2.2 Preparation of UiO-66-NH₂-ILBF₄⁻-Urea

UiO-66-NH₂ was prepared according the method reported in the literature [61, 62]. The prepared UiO-66-NH₂ (0.1 g) was dispersed in 10 mL DMF in a round-bottomed flask using sonication for 5 min. Next, (0.03 mmol, 10 mg) 1,3-bis-(4-bromo-butyl)-3*H*-imidazol-1-ium bromide was added to the mixture, and the solution was stirred under reflux for 24 h. Next, (0.06 mmol, 3.6 mg) urea was added to the mixture to form Task Specific Ionic Liquid (TSIL). After 24 h stirring under reflux, the precipitate was isolated by centrifugation. The product (UiO-66-NH₂-ILBr⁻-urea) was washed with DMF, water and ethanol. The supported ionic liquid phase was dried at 80 °C in an oven for 24 h. In the next step, an anion exchange was carried out by addition of sodium tetrafluoroborate (0.175 g, 1.5 mmol) to the solution of UiO-66-NH₂-ILBr⁻-urea (0.1 g) in acetone (2 mL) followed by stirred at room temperature for 24 h. The exchanged IL was then filtered and washed with H₂O (3 × 10 mL), EtOH (3 mL), Et₂O (2.5 mL), and acetone (2.5 mL). The resulting UiO-66-NH₂-ILBF₄⁻-urea was dried at 50 °C in an oven overnight to give the final product.

2.3 General Procedure for the Synthesis of Oximes

0.05 g of UiO-66-NH₂-ILBF₄⁻-urea dispersed in 1 mL ethanol was added to a mixture of benzaldehyde (1 mmol, 0.11 mL) and hydroxylamine hydrochloride (1.5 mmol, 0.1 g). Stirring at 25 °C (room temperature) was continued until the benzaldehyde was consumed, as monitored by thin layer chromatography (TLC). After completion of the reaction, the reaction mixture was added to 10 mL water and extracted with ether (3 × 10 mL). Further purification was accomplished by washing it with ethyl acetate and *n*-hexane. The organic products were identified by ¹H and ¹³C Nuclear Magnetic Resonance (NMR, Bruker 400 MHz) spectroscopy, by comparing with data in the literature [63]. The catalyst was washed with water and ethanol, and dried at 60 °C in an oven overnight. The catalyst was reused for several times under the same reaction conditions.

2.4 Spectral Data

2.4.1 Entry 1 (Benzaldehyde Oxime)

¹H NMR (400 MHz, *d*₆-DMSO): δ (ppm) 8.14 (s, 1H), 7.77–7.75 (d, 2H), 7.40–7.38 (m, 1H), 7.03–7.0 (dd, 2H); ¹³C NMR (100 MHz, *d*₆-DMSO): δ (ppm) 167.52, 151.64, 131.88, 129.71, 126.84, 118.02, 115.06.

2.4.2 Entry 2 (2-Hydroxybenzaldehyde Oxime)

¹H NMR (400 MHz, *d*₆-DMSO): δ (ppm) 8.33 (s, 1H), 7.49–7.47 (dd, 1H), 7.25–7.21 (dd, 1H), 6.90–6.86 (m, 2H); ¹³C NMR (100 MHz, *d*₆-DMSO): δ (ppm) 156.42, 147.96, 130.93, 128.30, 119.80, 118.72, 116.46.

2.4.3 Entry 3 (2-Methylbenzaldehyde Oxime)

¹H NMR (400 MHz, *d*₆-DMSO): δ (ppm) 8.29 (s, 1H), 7.67–7.64 (dd, 1H), 7.50–7.35 (td, 1H), 7.08–7.06 (d, 1H), 6.98–6.94 (t, 1H), 3.41 (s, 3H); ¹³C NMR (100 MHz, *d*₆-DMSO): δ (ppm) 157.26, 143.86, 131.23, 125.88, 121.38, 121.07, 112.19, 56.10. (Figure S10, Supporting Information).

2.4.4 Entry 4 (3,4,5-Trimethoxybenzaldehyde Oxime)

¹H NMR (400 MHz, CDCl₃): δ (ppm) 8.08 (s, 1H), 6.84 (s, 2H), 3.90 (s, 9H); ¹³C NMR (100 MHz, CDCl₃): δ (ppm) 153.48, 150.21, 139.71, 127.40, 104.12, 60.95, 56.18. (Figure S11, Supporting Information).

2.4.5 Entry 5 (Cinnamaldehyde Oxime)

¹H NMR (400 MHz, *d*₆-DMSO): δ (ppm) 7.58–7.56 (d, 1H), 7.42–7.39 (dd, 2H), 7.38–7.36 (t, 1H), 7.33–7.32 (dd, 2H), 7.29 (d, 1H), 6.98–6.95 (d, 1H); ¹³C NMR (100 MHz, *d*₆-DMSO): δ (ppm) 147.68, 138.35, 136.36, 129.50, 129.36, 127.67, 116.59.

2.4.6 Entry 6 (4-Nitrobenzaldehyde Oxime)

¹H NMR (400 MHz, *d*₆-DMSO): δ (ppm) 8.31 (s, 1H), 8.27–8.24 (dd, 2H), 7.88–7.84 (dd, 2H); ¹³C NMR (100 MHz, *d*₆-DMSO): δ (ppm) 147.97, 147.29, 139.96, 127.80, 124.45.

2.4.7 Entry 7 (3-Nitrobenzaldehyde Oxime)

¹H-NMR (400 MHz, *d*₆-DMSO): δ (ppm) 8.42–8.41 (t, 1H), 8.32 (s, 1H), 8.23–8.20 (dd, 1H), 8.06–8.03 (dd, 1H), 7.72–7.68 (t, 1H); ¹³C NMR (100 MHz, *d*₆-DMSO): δ (ppm) 148.57, 147.04, 135.39, 132.77, 130.79, 124.11, 121.26.

2.4.8 Entry 8 (2-Chlorobenzaldehyde Oxime)

¹H NMR (400 MHz, *d*₆-DMSO): δ (ppm) 8.37 (s, 1H), 7.83–7.81 (dd, 1H), 7.52–7.50 (dd, 1H), 7.45–7.42 (dd, 1H), 7.40–7.38 (dd, 1H); ¹³C NMR (100 MHz,

d_6 -DMSO): δ (ppm) 144.99, 132.64, 131.40, 130.74, 130.29, 128.01, 127.26.

2.4.9 Entry 9 (4-Methoxybenzaldehyde Oxime)

^1H NMR (400 MHz, d_6 -DMSO): δ (ppm) 8.06 (s, 1H), 7.96–7.93 (d, 1H), 7.53–7.51 (d, 1H), 7.31 (d, 1H), 6.99–6.95 (t, 1H), 3.79 (s, 3H); ^{13}C NMR (100 MHz, d_6 -DMSO): δ (ppm) 160.25, 148.07, 144.71, 132.76, 128.28, 114.64, 114.13, 55.66. (Figure S12, Supporting Information).

2.4.10 Entry 10 (Acetophenone Oxime)

^1H NMR (400 MHz, d_6 -DMSO): δ (ppm) 7.32–7.27 (dd, 2H), 7.21–7.19 (dd, 2H), 7.18 (t, 1H), 1.64 (s, 3H); ^{13}C NMR (100 MHz, d_6 -DMSO): δ (ppm) 155.05, 138.11, 128.90, 126.60, 13.50.

2.4.11 Entry 11 (Cyclohexanone Oxime)

^1H NMR (400 MHz, d_6 -DMSO): δ (ppm) 2.40–2.37 (t, 2H), 2.17–2.14 (m, 2H), 1.58–1.52 (m, 6H); ^{13}C NMR (100 MHz, d_6 -DMSO): δ (ppm) 159.35, 31.80, 27.03, 25.72, 24.53.

2.5 Characterization Techniques

Powder X-ray diffraction (PXRD) was used to study the crystalline nature of the MOF (UiO-66-NH₂) before and after modification (fresh and reused catalyst) by a Rigaku D-Max C III diffractometer (Cu K α , λ = 1.5418 Å). Infrared spectra were recorded by a Fourier transform infrared spectroscopy (FT-IR), from a Bruker vector 22 spectrometer,

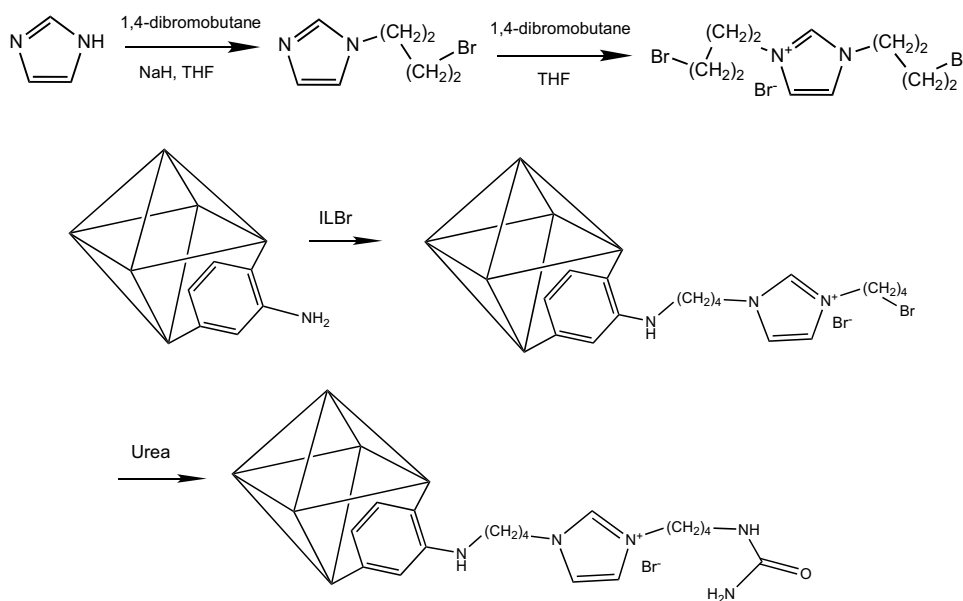
using KBr pellets. The chemical composition of the modified MOF was examined by a CHN elemental analyzer (Euro EA—HEKAtech GmbH) under N₂ gas flow and X-ray photoelectron spectroscopy (XPS) on a Kratos Axis Ultra-DLS spectrometer (Al K α source). The data was analyzed using the CasaXPS software. The thermal stability and organic species loading were studied by thermogravimetric analysis (TGA; Perkin Elmer STA 6000) at a heating rate of 10 °C min⁻¹ under nitrogen flow. The morphology and elemental analysis were carried out by a field emission scanning electron microscope (FE-SEM; FEI NOVA NanoSEM 450) equipped with energy dispersive X-ray spectroscopy (EDX). Platinum spurring was carried out on the samples before analysis to avoid undesirable electron charging. The BET (Brunauer–Emmett–Teller) specific surface area and adsorption BJH (Barrett–Joyner–Halenda) pore size/volume of the samples were measured by an automatic porosimeter (Micromeritics, Tristar II 3020). The samples were degassed under vacuum overnight before analysis. TEM images were acquired on a FEI Tecnai T20 G2 instrument at 200 kV from Thermo Fisher Scientific. Powdered samples were placed on holey carbon grids with no prior treatment.

3 Results and Discussion

3.1 Preparation and Characterization of UiO-66-NH₂-ILBr⁻-Urea Catalyst

After synthesizing the ionic liquid, 1,3-bis-(4-bromo-butyl)-3H-imidazol-1-ium bromide (ILBr⁻), the UiO-66-NH₂ was functionalized by ILBr⁻ and followed by urea. The reaction pathway to prepare UiO-66-NH₂-ILBr⁻-urea is given

Scheme 1 Preparation of ILBr⁻ and UiO-66-NH₂-ILBr⁻-urea



in Scheme 1. In addition, UiO-66-NH₂-ILBF₄⁻-urea was prepared via an anion exchange, Br⁻ replaced by BF₄⁻. The preparation steps were monitored by applying different characterization techniques.

XRD was used to study the crystalline structure of the UiO-66-NH₂ after functionalization by ILBr⁻ and grafting by urea (Fig. 1a). The characteristic diffraction of the UiO-66-NH₂ was observed at angles of 14.7°, 17.4°, 22.2°, 25.7°, 30.6°, 31.1°, 35.9°, 37.7°, 40.1°, 43.6°, 50.5°, and 56.8° corresponding to the (222), (400), (511), (600), (711), (731), (820), (751), (664), (933), (955), and (12 42) planes, respectively [64]. The UiO-66-NH₂-ILBF₄⁻-urea showed isostructural and similar pattern to that of the pristine MOF, indicating that the post-synthesis maintained the crystalline structure of the frameworks. Additional diffractions at 17.95°, 28.7°, 29.25°, and 47.9° were observed and could be attributed to IL-Urea.

The functionalization of the MOF was investigated by FT-IR (Fig. 1b). The characteristic peaks related to the N–H stretch of primary amines (3457 cm⁻¹ and 3351 cm⁻¹), carbonyl stretch (1661 cm⁻¹), C–N stretch (1259 cm⁻¹), and Zr–O stretch (600–800 cm⁻¹) were

observed [64]. A stretching vibration at 503 cm⁻¹ was attributed to CH₂–Br after attachment of ILBr⁻ to the ligand of the MOF. For UiO-66-NH₂-ILBF₄⁻-urea, the bands at 3370 and 3215 cm⁻¹ were related to the stretching vibration of N–H in amines, while the band at 1630 cm⁻¹ is attributed to the amide group in urea. Bands at 1590 cm⁻¹ and 1460 cm⁻¹ were assigned to the C=N and imidazolium ring, respectively.

Figure 1c, d demonstrated the N₂ adsorption–desorption isotherm and pore size distribution of the MOF. The isotherm showed a type IV hysteresis that is a characteristic pattern for mesoporous materials, while a fast adsorption at low pressure is consistent with microporous materials. Figure 1d showed a uniform distribution of the pore size in the framework. The surface area and porosity of the UiO-66-NH₂-ILBF₄⁻-urea were determined (Table 1). As expected, the surface area and pore size/volume were reduced after modification of UiO-66-NH₂. The BET surface area, total pore volume, and average pore size were obtained to be 600 m² g⁻¹, 0.39 cm³ g⁻¹, and 0.9 nm, respectively. The pore size of 0.9 nm belongs to the microporous materials according to the IUPAC classification of porous materials [65].

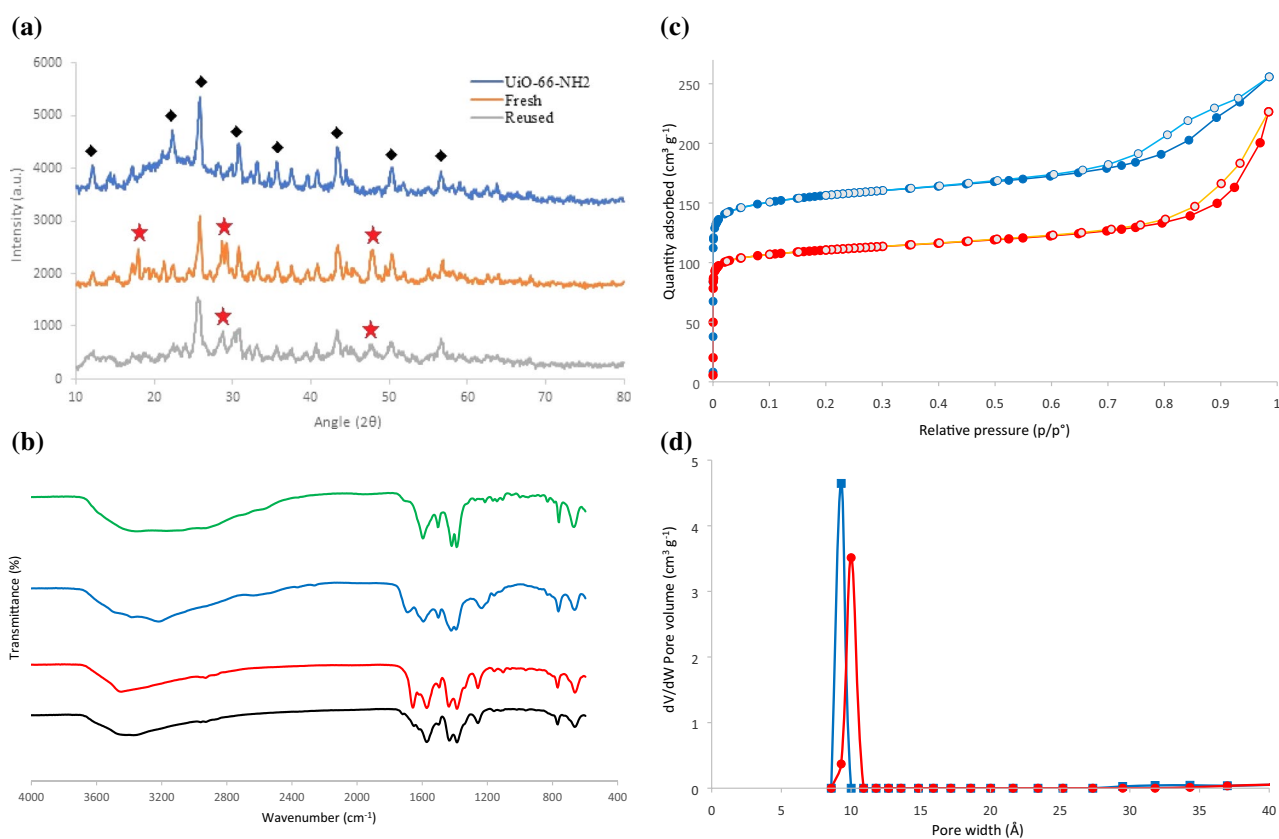


Fig. 1 **a** PXRD patterns of UiO-66-NH₂-ILBF₄⁻-urea in fresh and reused (after five times recycling), and **b** FT-IR spectra of UiO-66-NH₂ (black), UiO-66-NH₂-ILBr⁻ (red), fresh UiO-66-NH₂-ILBF₄⁻-urea (blue) and reused UiO-66-NH₂-ILBF₄⁻-urea (green).

c N₂ adsorption–desorption isotherm and **d** pore size distribution of the fresh (blue) and reused (red), after five times recycling, UiO-66-NH₂-ILBF₄⁻-urea. The solid spheres are referred to adsorption and the gray ones are for desorption

Table 1 Surface area and porosity of the UiO-66-NH₂-ILBF₄⁻-urea in fresh and recycled forms

	UiO-66-NH ₂	UiO-66-NH ₂ -ILBF ₄ ⁻ -urea (fresh)	UiO-66-NH ₂ -ILBF ₄ ⁻ -urea (recycled)
BET surface area (m ² g ⁻¹)	1280	601	427
Total pore volume (cm ³ g ⁻¹)	0.60	0.39	0.34
Average pore size (nm)	1.89	0.93	1.0

Table 2 Elemental compositions of the UiO-66-NH₂, UiO-66-NH₂-ILBr⁻ and UiO-66-NH₂-ILBr⁻-urea

MOFs	CHN (At%)		XPS (At%)				
	C	N	Zr	O	C	N	Br
UiO-66-NH ₂	21.28	4.49	2.88	31.47	60.72	4.84	–
UiO-66-NH ₂ -ILBr ⁻	24.28	5.65	2.41	23.32	64.07	2.60	7.60
UiO-66-NH ₂ -ILBr ⁻ -urea	18.39	3.48	7.61	30.12	37.46	0.9	23.90

CHN analysis was used to determine the amount of organic species loading on the surface of the MOFs (Table 2). The results showed that the content of carbon and nitrogen increased after modification of the UiO-66-NH₂ with ionic-liquid. The atomic percentage of carbon and nitrogen decreased after grafting urea to the ionic liquid, which can be related to the presence of heavy elements (i.e. Br) in the structure. XPS was also employed for detection of the elements and their quantities (Table 2). The presence of relevant elements (Zr, O, C, N, Br) in the structure of the MOF and the ionic liquid on the surface was verified. There is a difference in the elemental compositions obtained from CHN and XPS techniques due to their different operations applied for the analysis. In CHN, the content of selected elements (e.g. C, N, H) in the entire bulk of the samples is measured, while in XPS, almost all elements (except H) in the selected points of the samples in the surface and sub-layer with thickness < 10 nm is analyzed. Figures S7–S9 (Supporting Information) display the XPS surveys of UiO-66-NH₂, UiO-66-NH₂-ILBr⁻ and UiO-66-NH₂-ILBr⁻-urea, respectively. For UiO-66-NH₂ (Figure S5), the N 1s peak at 397 eV was attributed to NH₂ groups on the organic linkers. For the supported ILs, the O 1s peaks at 531 and 530.5 eV were assigned to the C=O groups in the linker and the urea, respectively (Figure S6 and S7), while the peak at 182 eV corresponded to the Br 3p in the C–Br bond (Figure S8). High-resolution XPS and the relevant deconvolution, in Fig. 2a, exhibited two components for the N peak. The peaks at ~401 and ~399.5 eV were assigned to the cationic N and the neutral N (–NH₂), respectively [66]. The peak at 401 eV confirms the presence of the imidazolium ring in the IL-supported UiO-66-NH₂ [67]. High-resolution XPS of the C 1s peak consists of three fitted peaks at binding energies of 283 and 284 and 290 eV (Fig. 2b). The peak at 283 eV was attributed to the C–C aliphatic (alkyl groups of the IL), while the peak at 284 eV was for C–N, C=C, and C=N

(in the linker and the imidazolium rings) [68]. The peak at 290 eV was also found to be correlated to the C=O in the linker and the urea [69].

The thermal stability and mass loading of ionic-liquid and urea into the framework were studied by TGA. In Fig. 3, The UiO-66-NH₂-ILBF₄⁻ and UiO-66-NH₂-ILBF₄⁻-urea showed almost similar thermal stability with the UiO-66-NH₂. An initial weight loss of ~ 5% and ~ 10% was found for UiO-66-NH₂-ILBF₄⁻ and UiO-66-NH₂-ILBF₄⁻-urea, respectively at below ~ 100 °C, while ~ 20% weight loss observed for the pristine MOF. The initial weight loss is related to the removal of the residual solvent (e.g. water and/or ethanol) from the pores. Moreover, an additional weight loss was observed at ~ 180–250 °C for the modified MOFs, relating to the escape of DMF coordinated to the nodes. Such event was not observed for the UiO-66-NH₂ because the MOF activation via a solvent extraction was efficient in removal of DMF. At temperature above 250 °C, slight reduction in the weight might be attributed to the thermal decomposition of the IL [70] and also urea groups in the modified MOFs, and removal of residual coordinated DMF inside the micropore of the UiO-66-NH₂ and partial degradation of the MOF structures ~ 400 °C. A further weight loss at ~ 500 °C was observed for the modified and pristine MOFs due to the framework degradation to ZrO₂ [64].

The TEM and SEM images (Fig. 4a, b) showed irregular round-shaped particles for UiO-66-NH₂-ILBF₄⁻-urea with sizes ranging from 50 to 100 nm. The EDS confirms the existence of the elements incorporated in the MOF (Fig. 4c). Zr (5.5%), O (17.3%), C (35.6%), N (7.6%), B (9.8%), and F (24.0%) were found. The result confirms the presence of B and F (corresponding to BF₄⁻) along with other elements in the structure. The trace amount of Br inferred an almost complete replacement of Br⁻ with BF₄⁻ within anion exchange. The elemental mapping demonstrated a homogeneous distribution of elements in the frameworks (Fig. 4d).

Fig. 2 High resolution XPS of **a** N 1s for UiO-66-NH₂-ILBr⁻ and **b** C 1s for UiO-66-NH₂-ILBr⁻-urea

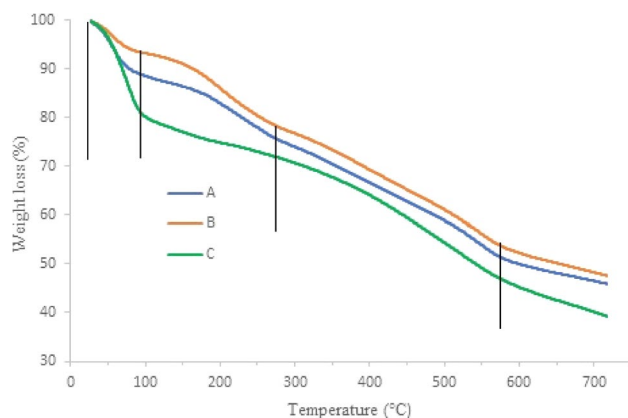
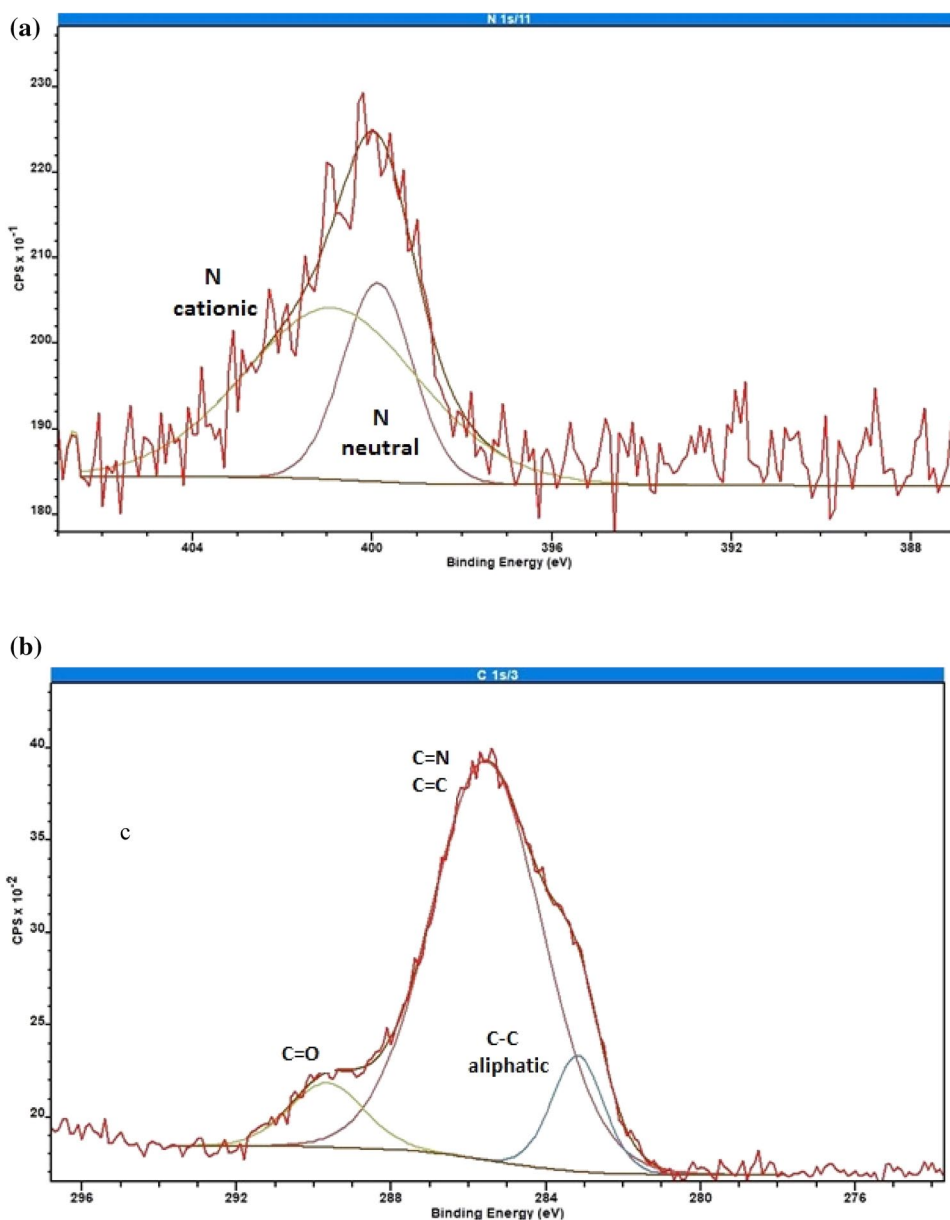


Fig. 3 Thermograms of (A) UiO-66-NH₂-ILBF₄⁻, (B) UiO-66-NH₂-ILBF₄⁻-urea, and (C) UiO-66-NH₂

3.2 Synthesis of Oximes Using UiO-66-NH₂-ILBF₄⁻-Urea Heterogeneous Catalyst

A zirconium MOF with incorporated IL and urea (UiO-66-NH₂-ILBF₄⁻-urea) was used as a platform for catalyzing organic reactions. In the current work, the synthesis of oximes was selected due to the simplicity of the procedure (highly crystalline compound [39]), an efficient condensation reaction, and an interesting intermediate with broad applications. Oxime is basically an imine with a general formula: RR'C=NOH, where R is an alkyl and R' could be hydrogen (to form aldoxime) and/or alkyl (to form ketoxime). The condensation reaction between benzaldehyde and hydroxylammonium chloride was chosen as a model reaction

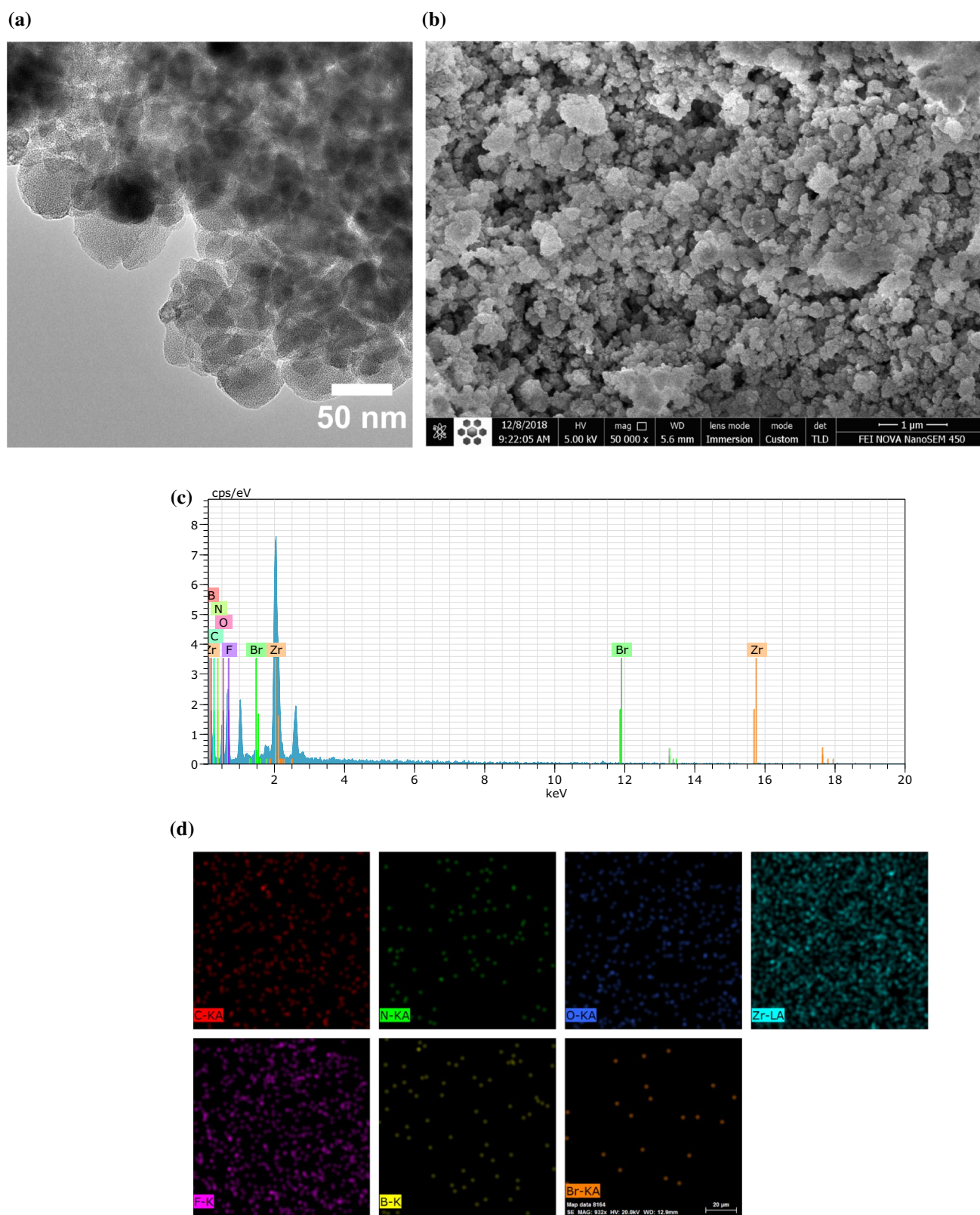


Fig. 4 TEM (a) and SEM (b) images, EDS spectrum (c), and elemental mapping in selected area (d) of the UiO-66-NH₂-ILBF₄⁻-urea

to examine the catalytic activity of UiO-66-NH₂-ILBF₄⁻-urea as a heterogeneous catalyst. Urea acts as a basic site for catalyzing the reaction and also adjust the pH of the medium to neutral as HCl is generated from hydroxylamine hydrochloride [42]. With regards to the mechanism, the amine group of urea initially activates the oxygen of the carbonyl group (of benzaldehyde) via a hydrogen bonding and facilitates the nucleophilic addition of hydroxylamine to the carbon of the carbonyl [42]. Two hydrogen bonding donors have been proposed for urea on the carbonyl activation [57]. Oxime is finally formed by a dehydration reaction.

To optimize the reaction conditions, the effect of various reaction parameters such as type of solvent, temperature, and amount of catalyst were studied in the first stage (Table 3). The effect of common solvents such as ethanol, acetonitrile, mixture of water and ethanol, and toluene were investigated on the reaction (Table 3, entry 1–3 and 6). The results revealed that a solvent with medium polarity of is indispensable for the reaction to proceed. Ethanol was found to be the best choice for this reaction. The effect of various temperatures such as (25, 60 and 90 °C) were studied for the model reaction (Table 3, entry 4–6). In contrast to the reported results, the lower temperature (25 °C) showed a better result compared to the higher temperatures. When the temperature was increased from 25 to 90 °C, the yield was decreased from 86 to 51% (Table 3, entry 4). It is proposed that the local motions of the linear and long alkyl group (attached to urea) increase by increasing the temperature leading to unfavorable interaction between urea and the imidazolium ring (synergic effect, discuss later). Hence, the urea (in cooperation with the IL) is not able to activate the carbonyl group of aldehydes and ketones for nucleophilic addition reaction. The effect of the catalyst amount on the reaction was also studied by varying it from 0.05–0.1 g (Table 3, entry 6–9), while keeping the other parameters

constant. It was observed that 0.05 g of catalyst was sufficient for completion of the reaction. It was observed that by using a higher amount of catalyst, the yield of the reaction was not enhanced. The optimum condition was found to be 0.05 g of the catalyst, ethanol as a solvent, temperature at 25 °C with a reaction time of 15 min.

To extent the current approach, a variety of substrates were used for the synthesis of different oximes. As shown in Table 4 various types of aromatic aldehydes with electron donating and withdrawing groups were successfully reacted with hydroxylamine hydrochloride and afforded the corresponding oximes in good to excellent yields. The nature of the substituents did not show a significant effect on the reaction efficiency, which is in good agreement with the results reported in the literature [71]. According to the results, hydroxy as an electron-donating group improved the reaction yield (Table 4, entry 2), while the alkyl and halide groups in the *ortho* position made a steric hindrance for the reaction and reduce the yield (Table 4, entries 3 and 8). Moreover, cinnamaldehyde as a non-aromatic showed a reasonable yield in the reaction (Table 4, entry 5). The nitro group in the *para* position (Table 4, entry 6) exhibited more deactivating effect in the condensation reaction compared to that in the *meta* position (Table 4, entry 7) due to an effective electron delocalization of the carbonyl group towards the nitro group in the *para* position. Methoxy groups in the *para* and *meta* positions showed unexpected results, compared to electron-donating and -withdrawing groups, for unknown reasons (Table 4, entries 4 and 9). On the other hand, aromatic ketones are generally less reactive in the condensation reaction compared to aromatic aldehydes due to their steric hindrance [50]. Acetophenone (Table 4, entry 10) exhibited a good yield (75% in 25 min) in comparison with the reported result with (55% yield in 10 min) using nanostructured pyrophosphate catalyst [71]. An aliphatic cyclic ketone, cyclohexanone (Table 4, entry 11), showed better results compared to aromatic ketones and comparable result with aromatic aldehydes.

The effect of anion incorporated on the IL (BF₄⁻ vs. Br⁻) was also studied by keeping the other parameters such as amount of catalyst, solvent type and temperature (Table 5). By replacing Br⁻ with BF₄⁻, the reaction time is reduced, and the reaction efficiency enhanced, which was consistent with the reported results; the IL of bmiBF₄ has showed higher yields compared to bmiCl [54]. Moreover, Br⁻ has a hydrophilic nature and is miscible in highly polar solvents, thus the ion solvation restricts the activity of the supported IL, in contrast BF₄⁻ exhibit hydrophobicity and immiscibility in aqueous media [73]. The effect of the substrate (i.e. UiO-66-NH₂) was examined and the result showed a medium activity probably due to high surface area and available basic sites on the MOF. In addition, the activity of the ionic liquid (e.g. ILBr⁻, IL-BF₄⁻) and urea in homogenous

Table 3 Optimization of the reaction conditions for the synthesis of oximes using UiO-66-NH₂-ILBF₄⁻-urea as the catalyst

Entry	Solvents	Catalyst amount (g)	Temperature (°C)	Yield (%) ^a
1	Toluene	0.05	25	43
2	Acetonitrile	0.05	25	50
3	Ethanol + H ₂ O	0.05	25	68
4	Ethanol	0.05	90	51
5	Ethanol	0.05	60	70
6	Ethanol	0.05	25	86
7	Ethanol	0.04	25	80
8	Ethanol	0.03	25	70
9	Ethanol	0.1	25	86

Reaction conditions: benzaldehyde (1 mmol), hydroxylammonium chloride (1.5 mmol), solvent (1 mL), catalyst, reaction time (15 min)

^aIsolated yield

Table 4 Synthesis of oximes via reaction of aldehydes and/or ketones with hydroxylammonium chloride

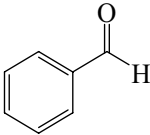
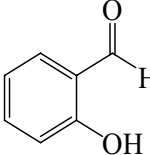
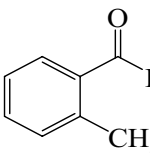
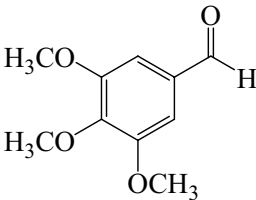
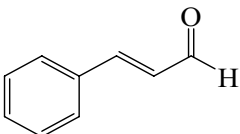
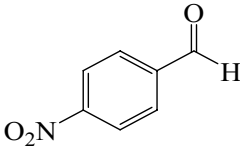
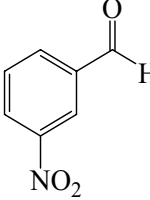
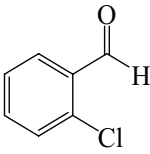
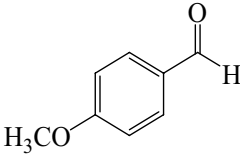
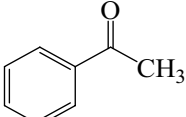
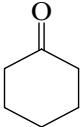
Entry	Substrate	Time (min)	Yield (%) ^a	Melting point (°C) [Ref.]
1		15	86	31–33 (33–35) [56]
2		25	92	55–58 (57–59) [56]
3		25	82	57–59 (51–53) [72]
4		30	67	178–182
5		25	78	132–136 (136–138) [56]
6		30	77	126–128 (128–130) [56]
7		30	83	116–118 (116–118) [42]
8		30	61	63–65 (68–72) [42]

Table 4 (continued)

Entry	Substrate	Time (min)	Yield (%) ^a	Melting point (°C) [Ref.]
9		35	65	131–133 (131–133) [56]
10		25	75	56–57 (56–59) [42]
11		20	83	80–85 (84–85) [42]

Reaction conditions: aldehyde or ketone (1 mmol), hydroxylammonium chloride (1.5 mmol), ethanol (1 mL), UiO-66-NH₂-ILBF₄⁻-urea (0.05 g) at 25 °C in 15–35 min

^aIsolated yield

Table 5 The catalytic activity of the catalyst, the support and the IL in homogeneous phase

Catalyst	Time (min)	Yield (%) ^a
UiO-66-NH ₂ -ILBF ₄ ⁻ -urea	15	86
UiO-66-NH ₂ -ILBr ⁻ -urea	20	70
UiO-66-NH ₂	30	43
ILBF ₄ ⁻	35	33
ILBr ⁻	35	20
Urea	35	Trace

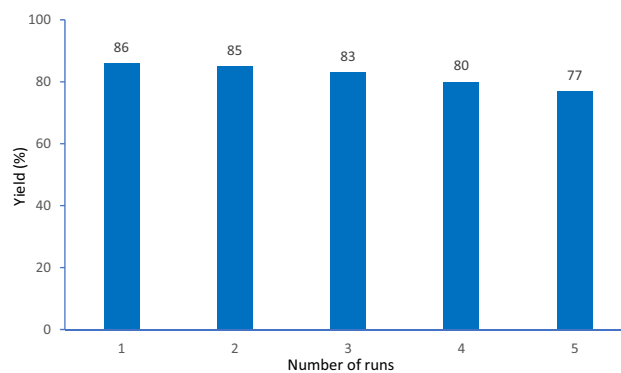
Reaction conditions: benzaldehyde (1 mmol), hydroxylammonium chloride (1.5 mmol), ethanol (1 mL), temperature (25 °C), and catalyst or UiO-66-NH₂ or IL (0.05 g)

^aIsolated yield

phase were investigated. ILs exhibited a limited effect on the activation of the carbonyl groups and deprotonation of hydroxyl amine by Br⁻ and BF₄⁻. Urea as a base was not effective in the homogeneous phase, while by grafting to the IL and the MOF, their synergic effects may promote the hydrogen-bonding donation of the urea in heterogeneous phase. A similar synergic activation has been found for (2-hydroxyethyl)trimethylammonium in choline chloride/urea system supported on molecular sieves for the CO₂ cyclization with epoxides [74].

3.2.1 Catalyst Recycling and Stability

The recyclability and reusability of the catalyst were studied for the condensation reaction using a model reaction between benzaldehyde with hydroxylammonium chloride

**Fig. 5** Reusability of the catalyst for the synthesis of oxime

(Fig. 5). After each cycle, the catalyst was reactivated by centrifugation, washing with water and ethanol (to remove the residual starting materials on the catalyst surface and pores), and drying at 60 °C in an oven overnight. The catalyst was successfully recycled and reused 5 times without significant loss of the performance. The slight reduction in catalyst activity might be related to the partial blocking of the pores by trapped starting materials or product [75, 76]. The BET surface area and total pore volume of the reused catalyst were reduced (*cf.* the fresh catalyst) and found to be 427 m² g⁻¹ and 0.34 cm³ g⁻¹, respectively, although a slight increase in pore size (1.0 nm) was observed (Table 1). The N₂ adsorption–desorption isotherm and pore size distribution of the reused catalyst can be found in Fig. 1c, d.

The catalyst stability was investigated by XRD, FTIR, electron microscopy, and elemental analysis. XRD pattern

and the FT-IR spectrum of the reused UiO-66-NH₂-ILBF₄⁻-urea show similar patterns (Fig. 1a, b) to those in fresh catalyst, indicating that the catalyst is almost stable under reaction conditions after five times of recycling and reusing. Furthermore, the morphology and the chemical composition of the UiO-66-NH₂-ILBF₄⁻-urea (after five times of reusing) were studied by FE-SEM (Fig. 6) and elemental analysis/mapping (Figure S8 and S9, Supporting Information). The results showed a slight change in the morphology and similar

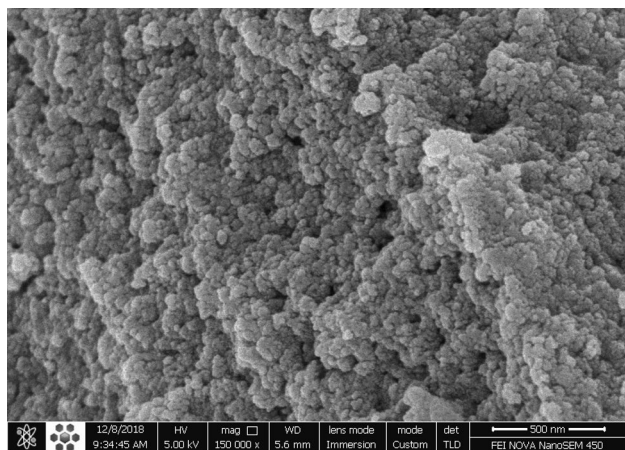


Fig. 6 FE-SEM image of the catalyst after five times reuse

composition for the recycled catalyst in comparison with those for the fresh catalyst. An atomic percentage for the corresponding elements in the recycled catalyst was found to be Zr (4.4%), O (18.6%), C (39.1%), N (5.2%), B (9.3%), and F (23.3%). A slight reduction in the content of B and F (corresponding to BF₄⁻) caused negligible leaching for the reused catalyst after five successive recycling. Furthermore, the activity of the extracted catalyst after hot filtration (70 °C in EtOH for 2 h) was reduced to a yield of 80%, which could be related to leaching of BF₄⁻ at an elevated temperature. Consequently, the catalyst can be easily recycled and reused several times with a reasonable stability.

Different types of acidic (Brønsted, Lewis, and solid acids, entries 1–11, Table 6) and basic (metal hydroxide and organic bases, entries 12–15) conditions were used for the synthesis of oximes. Organic and polar solvents and also solventless conditions were suitable media for the syntheses. Microwave (MW) and ultrasonic (US) irradiations, reflux, and grinding were applied to accelerate the reactions. Ionic liquids were also employed as a catalyst or reaction medium. Major environmental and economic concerns on the reported catalytic systems are catalyst recoverability and reusability, therefore, integration of catalysts to solid porous supports is encouraging. The current catalytic system, a heterogeneous basic catalyst, showed comparable results in terms of yield and reaction conditions (e.g. temperature and time), and

Table 6 Synthesis of oximes via reaction of benzaldehydes with hydroxylammonium chloride (NH₂OH.HCl) using different catalytic systems

Entry	Catalytic systems	Reaction conditions	Time (min)	Yield (%)	Ref
1	TiO ₂ /SO ₄ ²⁻ (0.05 g)	130 °C, solventless	1	100	[50]
2	Na ₂ SO ₄ (0.1 mmol)	US (25–35 °C), EtOH	5	88	[42]
3	HCl (2 drops), K ₂ CO ₃ (10%), pH 10	US, H ₂ O	Immediately	91	[77]
4	BF ₃ ·Et ₂ O (10 mol%)	Reflux, CH ₃ OH	3.5 (h)	87 ^a	[43]
5	BF ₃ ·Et ₂ O (10 mol%)	MW, CH ₃ OH	6	95 ^a	[43]
6	Silica gel 60, 230–400 mesh (1 g)	MW (800 W, 80–90 °C), solventless	3	100	[39]
7	Wet basic Al ₂ O ₃ (1.5 equiv.)	MW, solventless	5	79	[52]
8	Molecular sieves 4 Å (2.5 g)	Grinding	30	60	[52]
9	Na ₂ CaP ₂ O ₇ nanostructure (0.1 g)	MW (400 W, 80 °C), solventless	4	82	[71]
10	Na ₂ CaP ₂ O ₇ nanostructure (0.1 g)	80 °C, solventless	10	83	[71]
11	Na ₁₂ [WZn ₃ (H ₂ O) ₂ (ZnW ₉ O ₃₄) ₂] (0.01 mmol)	H ₂ O ₂ (27%), NH ₃ (25%), H ₂ O, rt	6 (h)	95	[51]
12	NaOH (1.2 mol)	Grinding, CH ₃ OH (2–4 drops), rt	2	71 ^b	[53]
13	DABCO ^c (1 mmol)	Grinding and MW (900 W), solventless	70 (s)	98	[56]
14	(PhCH ₂) ₃ N (1 mmol)	Grinding and MW (900 W), solventless	90	98	[56]
15	Glycine (0.5 mmol)	DMF, rt	5 (h)	96 ^d	[58]
16	[bmIm]OH (2 mmol)	US, EtOH, rt	5	91	[55]
17	bmiBF ₄ (2 mmol)	rt	30	95 ^d	[54]
18	UiO-66-NH ₂ -ILBF ₄ ⁻ -urea (0.05 g)	EtOH, rt	15	86	This work

^aCH₃CONHOH was used instead of NH₂OH·HCl

^b2-Hydroxybenzaldehyde as a precursor

^c1,4-Diazabicyclo[2.2.2]octane

^dCyclohexane as a precursor

superior recyclability, reusability, and robustness compared to the reported systems.

4 Conclusion

A robust supported ionic liquid system is introduced for the organic synthesis of oximes. In the design strategy, the basic heterogeneous catalyst was successfully prepared by employing a chemical/thermal stable Zr-based MOF, UiO-66-NH₂ as a support. The MOF was initially modified with an ionic liquid to make a supported ionic liquid (SIL), followed by covalent anchoring of urea to the cation moiety of IL to form a TSIL. The as-prepared catalyst was examined for the synthesis of oximes. UiO-66-NH₂-ILBF₄⁻-urea catalyst showed excellent performance in the reaction of various aldehydes and ketones with hydroxylammonium chloride in good yields. Ethanol was the best candidate as a solvent in the current method. The catalyst was successfully recycled and reused for several times without significant loss of activity. Due to high specific area and large porosity of the MOFs, they can be extensively employed in various catalytic reactions with efficient performance. Moreover, a large number of available pores in MOFs can be a suitable host for ionic liquids to produce a large variety of heterogeneous catalysts. More efforts can be helpful to design new task-specific ILs attached to MOF using basic groups (e.g. thiourea, polyamines, etc.) and/or acidic groups (e.g. -SO₃H).

Acknowledgements M. Jafarzadeh is thankful to Razi University for the partial financial supports, and Prof. Kim Daasbjerg and Monica Rohde Madsen (Aarhus University, Denmark) for XPS analysis.

References

- Campisciano V, Giacalone F, Gruttadauria M (2017) Supported ionic liquids: a versatile and useful class of materials. *Chem Rec* 17:918–938
- Romanovsky BV, Tarkhanova IG (2017) Supported ionic liquids in catalysis. *Russ Chem Rev* 86:444–458
- Riisager A, Jørgensen B, Wasserscheid P, Fehrmann R (2006) First application of supported ionic liquid phase (SILP) catalysis for continuous methanol carbonylation. *Chem Commun* 9:994–996
- Joni J, Haumann M, Wasserscheid P (2009) Development of a supported ionic liquid phase (SILP) catalyst for slurry-phase Friedel-Crafts alkylations of cumene. *Adv Synth Catal* 351:423–431
- Lemus J, Palomar J, Gilarranz MA, Rodriguez JJ (2011) Characterization of supported ionic liquid phase (SILP) materials prepared from different supports. *Adsorption* 17:561–571
- More S, Jadhav S, Salunkhe R, Kumbhar A (2017) Palladium supported ionic liquid phase catalyst (Pd@SILP-PS) for room temperature Suzuki-Miyaura cross-coupling reaction. *Mol Catal* 442:126–132
- Xin B, Hao J (2014) Imidazolium-based ionic liquids grafted on solid surfaces. *Chem Soc Rev* 43:7171–7187
- Riisager A, Fehrmann R, Haumann M, Wasserscheid P (2006) Supported ionic liquid phase (SILP) catalysis: An innovative concept for homogeneous catalysis in continuous fixed-bed reactors. *Eur J Inorg Chem* 2006:695–706
- Zhang Q, Zhang S, Deng Y (2011) Recent advances in ionic liquid catalysis. *Green Chem* 13:2619–2637
- Hagiwara H, Sekifuji M, Hoshi T, Qiao K, Yokoyama C (2007) Synthesis of bis(indolyl)methanes catalyzed by acidic ionic liquid immobilized on silica (ILIS). *Synlett* 2007:1320–1322
- Gu Y, Li G (2009) Ionic liquids-based catalysis with solids: state of the art. *Adv Synth Catal* 351:817–847
- Lee S-G (2006) Functionalized imidazolium salts for task-specific ionic liquids and their applications. *Chem Commun* 10:1049–1063
- Olivier-Bourbigou H, Magna L, Morvan D (2010) Ionic liquids and catalysis: Recent progress from knowledge to applications. *Appl Catal A* 373:1–56
- Sawant AD, Raut DG, Darvatkar NB, Salunkhe MM (2011) Recent developments of task-specific ionic liquids in organic synthesis. *Green Chem Lett Rev* 4:41–54
- Izák P, Bobbink FD, Hulla M, Klepic M, Friess K, Hovorka S, Dyson PJ (2018) Catalytic ionic-liquid membranes: the convergence of ionic-liquid catalysis and ionic-liquid membrane separation technologies. *ChemPlusChem* 83:7–18
- Mehnert CP (2005) Supported ionic liquid catalysis. *Chem Eur J* 11:50–56
- Mehnert CP, Cook RA, Dispenziere NC, Afeworki M (2002) Supported ionic liquid catalysis—a new concept for homogeneous hydroformylation catalysis. *J Am Chem Soc* 124:12932–12933
- Li H, Bhadury PS, Song B, Yang S (2012) Immobilized functional ionic liquids: efficient, green, and reusable catalysts. *RSC Adv* 2:12525–12551
- Luo Q-X, An B-W, Ji M, Zhang J (2018) Hybridization of metal-organic frameworks and task-specific ionic liquids: fundamentals and challenges. *Mater Chem Front* 2:219–234
- Takashima Y, Yokoyama M, Horikoshi A, Sato Y, Tsuruoka T, Akamatsu K (2017) Ionic liquid/metal-organic framework hybrid generated by ion-exchange reaction: synthesis and unique catalytic activity. *New J Chem* 41:14409–14413
- Farrusseng D, Aguado S, Pinel C (2009) Metal-organic frameworks: Opportunities for catalysis. *Angew Chem Int Ed* 48:7502–7513
- He H, Perman JA, Zhu G, Ma S (2016) Metal-organic frameworks for CO₂ chemical transformations. *Small* 12:6309–6324
- Jiao L, Seow JYR, Skinner WS, Wang ZU, Jiang H-L (2019) Metal-organic frameworks: structures and functional applications. *Mater Today* 27:43–68
- Luo Q-X, Ji M, Lu M-H, Hao C, Qiu J-S, Li Y-Q (2013) Organic electron-rich N-heterocyclic compound as a chemical bridge: building a Brønsted acidic ionic liquid confined in MIL-101 nanocages. *J Mater Chem A* 1:6530–6534
- Luo Q-X, Ji M, Park S-E, Hao C, Li Y-Q (2016) PdCl₂ immobilized on metal-organic framework CuBTC with the aid of ionic liquids: enhanced catalytic performance in selective oxidation of cyclohexene. *RSC Adv* 6:33048–33054
- Abednatanzi S, Leus K, Gohari Derakhshandeh P, Nahra F, De Keukeleere K, Van Hecke K, Van Driessche I, Abbasi A, Nolan SP, Van Der Voort P (2017) POM@IL-MOFs—inclusion of POMs in ionic liquid modified MOFs to produce recyclable oxidation catalysts. *Catal Sci Technol* 7:1478–1487
- Abednatanzi S, Abbasi A, Masteri-Farahani M (2017) Immobilization of catalytically active polyoxotungstate into ionic liquid-modified MIL-100(Fe): a recyclable catalyst for selective oxidation of benzyl alcohol. *Catal Commun* 96:6–10
- Khan NA, Hasan Z, Jhung SH (2014) Ionic liquids supported on metal-organic frameworks: remarkable adsorbents for adsorptive desulfurization. *Chem Eur J* 20:376–380

29. Wu J, Gao Y, Zhang W, Tan Y, Tang A, Men Y, Tang B (2015) Deep desulfurization by oxidation using an active ionic liquid-supported Zr metal-organic framework as catalyst. *Appl Organometal Chem* 29:96–100
30. Luo Q-X, Song X-D, Ji M, Park S-E, Hao C, Li Y-Q (2014) Molecular size- and shape-selective Knoevenagel condensation over microporous Cu₃(BTC)₂ immobilized amino-functionalized basic ionic liquid catalyst. *Appl Catal A* 478:81–90
31. Tharun J, Bhin K-M, Roshan R, Kim DW, Kathalikkattil AC, Babu R, Ahn HY, Won YS, Park D-W (2016) Ionic liquid tethered post functionalized ZIF-90 framework for the cycloaddition of propylene oxide and CO₂. *Green Chem* 18:2479–2487
32. Ding L-G, Yao B-J, Jiang W-L, Li J-T, Fu Q-J, Li Y-A, Liu Z-H, Ma J-P, Dong Y-B (2017) Bifunctional imidazolium-based ionic liquid decorated UiO-67 type MOF for selective CO₂ adsorption and catalytic property for CO₂ cycloaddition with epoxides. *Inorg Chem* 56:2337–2344
33. Ma D, Li B, Liu K, Zhang X, Zou W, Yang Y, Li G, Shi Z, Feng S (2015) Bifunctional MOF heterogeneous catalysts based on the synergy of dual functional sites for efficient conversion of CO₂ under mild and co-catalyst free conditions. *J Mater Chem A* 3:23136–23142
34. Wu Z, Chen C, Wan H, Wang L, Li Z, Li B, Guo Q, Guan G (2016) Fabrication of magnetic NH₂-MIL-88B (Fe) confined Brønsted ionic liquid as an efficient catalyst in biodiesel synthesis. *Energy Fuels* 30:10739–10746
35. Yang SH, Chang S (2001) Highly efficient and catalytic conversion of aldoximes to nitriles. *Org Lett* 3:4209–4211
36. Park S, Choi Y-A, Han H, Yang SH, Chang S (2003) Rh-Catalyzed one-pot and practical transformation of aldoximes to amides. *Chem Commun* 15:1936–1937
37. Peng H-G, Xu L, Wu H, Zhang K, Wu P (2013) One-pot synthesis of benzamide over a robust tandem catalyst based on center radially fibrous silica encapsulated TS-1. *Chem Commun* 49:2709–2711
38. Klitgaard SK, Egeblad K, Mentzel UV, Popov AG, Jensen T, Taarning E, Nielsen IS, Christensen CH (2008) Oxidations of amines with molecular oxygen using bifunctional gold–titania catalysts. *Green Chem* 10:419–423
39. Hajipour AR, Mallakpour SE, Imanzadeh G (1999) A rapid and convenient synthesis of oximes in dry media under microwave irradiation. *J Chem Res (S)* 3:228–229
40. Hajipour AR, Mallakpour SE, Khoei S (2002) An easy and fast method for conversion of oximes to the corresponding carbonyl compounds under microwave irradiation. *Synth Commun* 32:9–15
41. Kukushkin VY, Pombeiro AJL (1999) Oxime and oximate metal complexes: unconventional synthesis and reactivity. *Coord Chem Rev* 181:147–175
42. Li J-T, Li X-L, Li T-S (2006) Synthesis of oximes under ultrasound irradiation. *Ultrason Sonochem* 13:200–202
43. Sridhar M, Narsaiah C, Raveendra J, Reddy GK, Reddy MKK, Ramanaiah BC (2011) Efficient microwave-assisted synthesis of oximes from acetohydroxamic acid and carbonyl compounds using BF₃·OEt₂ as the catalyst. *Tetrahedron Lett* 52:4701–4704
44. Sha Q, Wei Y (2013) Base and solvent mediated decomposition of tosylhydrazones: highly selective synthesis of N-alkyl substituted hydrazones, dialkylidenehydrazines, and oximes. *Tetrahedron* 69:3829–3835
45. Yu J, Lu M (2015) Copper(II)-promoted direct conversion of methylarenes into aromatic oximes. *Org Biomol Chem* 13:7397–7401
46. Yu J, Jin Y, Lu M (2015) 3-Methyl-4-oxa-5-azahomoadamantane as an organocatalyst for the aerobic oxidation of primary amines to oximes in water. *Adv Synth Catal* 357:1175–1180
47. Xue X, Song F, Ma B, Yu Y, Li C, Ding Y (2013) Selective ammoximation of ketones and aldehydes catalyzed by a trivanadium-substituted polyoxometalate with H₂O₂ and ammonia. *Catal Commun* 33:61–65
48. Xing S, Han Q, Shi Z, Wang S, Yang PP, Wu Q, Li M (2017) A hydrophilic inorganic framework based on a sandwich polyoxometalate: unusual chemoselectivity for aldehydes/ketones with *in situ* generated hydroxylamine. *Dalton Trans* 46:11537–11541
49. Hyodo K, Togashi K, Oishi N, Hasegawa G, Uchida K (2016) Brønsted acid catalyzed transoximation reaction: synthesis of aldoximes and ketoximes without use of hydroxylamine salts. *Green Chem* 18:5788–5793
50. Guo J-J, Jin T-S, Zhang S-L, Li T-S (2001) TiO₂/SO₄²⁻: an efficient and convenient catalyst for preparation of aromatic oximes. *Green Chem* 3:193–195
51. Sloboda-Rozner D, Neumann R (2006) Aqueous biphasic catalysis with polyoxometalates: oximation of ketones and aldehydes with aqueous ammonia and hydrogen peroxide. *Green Chem* 8:679–681
52. Kad GL, Bhandari M, Kaur J, Rathee R, Singh J (2001) Solventless preparation of oximes in the solid state and via microwave irradiation. *Green Chem* 3:275–277
53. Aakeröy CB, Sinha AS, Epa KN, Spartz CL, Desper J (2012) A versatile and green mechanochemical route for aldehyde–oxime conversions. *Chem Commun* 48:11289–11291
54. Ren RX, Ou W (2001) Preparation of cyclic ketoximes using aqueous hydroxylamine in ionic liquids. *Tetrahedron Lett* 42:8445–8446
55. Zang H, Wang M, Cheng B-W, Song J (2009) Ultrasound-promoted synthesis of oximes catalyzed by a basic ionic liquid [bmIm]OH. *Ultrason Sonochem* 16:301–303
56. Hajipour AR, Rafiee F, Ruoho AE (2010) A rapid and convenient method for the synthesis of aldoximes under microwave irradiation using *in situ* generated ionic liquids. *J Iran Chem Soc* 7:114–118
57. Taylor MS, Jacobsen EN (2006) Asymmetric catalysis by chiral hydrogen-bond donors. *Angew Chem Int Ed* 45:1520–1543
58. Maheswara M, Siddaiah V, Gopalaiiah K, Rao VM, Rao CV (2006) A simple and effective glycine-catalysed procedure for the preparation of oximes. *J Chem Res* 2006:362–363
59. Vitz J, Mac DH, Legoupy S (2007) Ionic liquid supported tin reagents for Stille cross coupling reactions. *Green Chem* 9:431–433
60. Zhang Y, Zhen B, Li H, Feng Y (2018) Basic ionic liquid as catalyst and surfactant: green synthesis of quinazolinone in aqueous media. *RSC Adv* 8:36769–36774
61. Kandiah M, Nilsen MH, Usseglio S, Jakobsen S, Olsbye U, Tilset M, Larabi C, Quadrelli EA, Bonino F, Lillerud KP (2010) Synthesis and stability of tagged UiO-66 Zr-MOFs. *Chem Mater* 22:6632–6640
62. Katz MJ, Brown ZJ, Colón YJ, Siu PW, Scheidt KA, Snurr RQ, Hupp JT, Farha OK (2013) A facile synthesis of UiO-66, UiO-67 and their derivatives. *Chem Commun* 49:9449–9451
63. Zhang L, Chen H, Zha Z, Wang Z (2012) Electrochemical tandem synthesis of oximes from alcohols using KNO₃ as the nitrogen source, mediated by tin microspheres in aqueous medium. *Chem Commun* 28:6574–6576
64. Hinde CS, Webb WR, Chew BKJ, Tan HR, Zhang W-H, Hor TSA, Raja R (2016) Utilisation of gold nanoparticles on amine-functionalised UiO-66 (NH₂-UiO-66) nanocrystals for selective tandem catalytic reactions. *Chem Commun* 52:6557–6560
65. Thommes M, Kaneko K, Neimark AV, Olivier JP, Rodriguez-Reinoso F, Rouquerol J, Sing KSW (2015) Physisorption of gases, with special reference to the evaluation of surface area and pore size distribution (IUPAC technical report). *Pure Appl Chem* 87:1051–1069
66. Sui Z-Y, Cui Y, Zhu J-H, Han B-H (2013) Preparation of three-dimensional graphene oxide–polyethylenimine porous

- materials as dye and gas adsorbents. *ACS Appl Mater Interfaces* 5:9172–9179
67. Beattie DA, Arcifa A, Delcheva I, Le Cerf BA, MacWilliams SV, Rossi A, Krasowska M (2018) Adsorption of ionic liquids onto silver studied by XPS. *Colloids Surf A* 544:78–85
 68. Li X, Sui Z-Y, Sun Y-N, Xiao P-W, Wang X-Y, Han B-H (2018) Polyaniline-derived hierarchically porous nitrogen-doped carbons as gas adsorbents for carbon dioxide uptake. *Microporous Mesoporous Mater* 257:85–91
 69. Xiao P-W, Zhao L, Sui Z-Y, Han B-H (2017) Synthesis of core-shell structured porous nitrogen-doped carbon@silica material via a sol-gel method. *Langmuir* 33:6038–6045
 70. Gupta R, Yadav M, Gaur R, Arora G, Sharma RK (2017) A straightforward one-pot synthesis of bioactive *N*-aryl oxazolidin-2-ones via a highly efficient Fe₃O₄@SiO₂-supported acetate-based butylimidazolium ionic liquid nanocatalyst under metal- and solvent-free conditions. *Green Chem* 19:3801–3812
 71. Elmakssoudi A, Abdelouahdi K, Zahouily M, Clark J, Solhy A (2012) Efficient conversion of aldehydes and ketones into oximes using a nanostructured pyrophosphate catalyst in a solvent-free process. *Catal Commun* 29:53–57
 72. Ribeiro TS, Prates A, Alves SR, Oliveira-Silva JJ, Riehl CAS, Figueroa-Villar JD (2012) The effect of neutral oximes on the reactivation of human acetylcholinesterase inhibited with paraoxon. *J Braz Chem Soc* 23:1216–1225
 73. Van Doorslaer C, Wahlen J, Mertens P, Binnemans K, De Vos D (2010) Immobilization of molecular catalysts in supported ionic liquid phases. *Dalton Trans* 39:8377–8390
 74. Zhu A, Jiang T, Han B, Zhang J, Xie Y, Ma X (2007) Supported choline chloride/urea as a heterogeneous catalyst for chemical fixation of carbon dioxide to cyclic carbonates. *Green Chem* 9:169–172
 75. Corma A, García H, Llabrés i Xamena FX (2010) Engineering metal organic frameworks for heterogeneous catalysis. *Chem Rev* 110:4606–4655
 76. Chen J, Shen K, Li Y (2017) Greening the processes of metal-organic framework synthesis and their use in sustainable catalysis. *Chemsuschem* 10:3165–3187
 77. Khoramabadi-Zad A, Azadmanesh M, Rezaee A (2010) Simple, Efficient and green synthesis of oximes under ultrasound irradiation. *S Afr J Chem* 63:192–194

Publisher's Note Springer Nature remains neutral with regard to jurisdictional claims in published maps and institutional affiliations.

Affiliations

Saeed Askari¹ · Mohammad Jafarzadeh¹ · David Benjamin Christensen² · Søren Kegsnæs²

¹ Faculty of Chemistry, Razi University, 67144-14971 Kermanshah, Iran

² Department of Chemistry, Technical University of Denmark, 2800 Kgs. Lyngby, Denmark